

# Orbital Analysis of a Breathing Cracked Rotor During its Passage Through the Subcritical Speeds

Otmane Zerrouki <sup>1,\*</sup>, Ahmed Fellah <sup>1</sup> and Ahmed Saimi <sup>2</sup>

<sup>1</sup> Mechanical department, Faculty of science and technology, University of Relizane, Algeria

<sup>2</sup> IS2M laboratory, Faculty of technology, University of Tlemcen, Algeria

**Abstract.** In the present paper, an orbital analysis is conducted to study the effect of a transverse breathing crack on the orbits of the rotor during its passage through the subcritical speeds; this study makes it possible to predict the presence of cracks in rotors. The classical version of the finite element method is used to model the rotor. While, the equation of motion is obtained by the application of the Lagrange equation on the kinetic and deformation energies of the different components of the rotor taking into account the variation of the shaft's stiffness due to the crack, The results are obtained using a Matlab code based on Newmark's beta method, this program allows us to plot the orbits of the rotor centre during its passage through the subcritical speeds.

**Keywords:** Rotor, Breathing Crack, FEM, Orbit, Subcritical Speed.

## 1. Introduction

Rotors have extensive applications in many industrial machines; they are widely used in turbines, compressors, pumps, motors ... etc. Continuous loads on the rotors can lead to unpredictable damage and failure such as cracks. This damage leads to dangerous, destructive and catastrophic scenarios.

Over the past three decades, many researchers have worked and provided theoretical and experimental work to study the dynamics of cracked and uncracked rotors. Comments on cracked rotors can be found [1-3]. In addition, the finite element stiffness matrix of the cracked element of a cracked rotor was determined, using the flexibility matrix method. As a result, the finite element model (FEM) was formulated and solved for studying the dynamic behaviour of the cracked rotor system [4-9].

Studies on multiple faults were also conducted in [10] and [11] where different techniques were employed to study the faults including frequency response and whirl orbits analysis. In the remaining part of this introduction, the impact of typical faults in rotor systems on shaft's whirling in its whirl orbit is reviewed.

The breathing and the open model of the transverse crack are considered to be the main theories to study the vibratory behaviour of cracked rotor systems. Since the breathing crack causes asymmetry in the shaft cross section, the principle of asymmetric bending should be utilized for accurate modeling of the breathing behaviour, in which the neutral axis will be inclined with changing the rotational angles, instead of the assumed horizontal neutral axis as developed [12]. Several people since the 1970s [13–16] have considered the stiffness change due to a crack and incorporated this into the equations of motion, in the form of a time-periodic function changing between the maximum stiffness value for the fully closed crack status and a minimum value for the

fully open crack status. [17] expressed the equation of motion with the response-dependent stiffness in a simple rotor. [18] evaluated the dynamic response of the rotor with a breathing crack by expanding the changing stiffness of the crack in a truncated Fourier series and using the Harmonic Balance Method. The dynamic behaviour of the whirl orbits in the neighbourhood of the subcritical rotational speeds or during the passage through these speeds was studied in [19-22] for a cracked rotor with a breathing crack model

The orbits during transient operation at the critical speed and at half of the critical speed were considered to be the unique characteristics of the cracked rotor system. Babu, et al. [23] analysed the coupling of the longitudinal and lateral steady state vibrations of a cracked Jeffcott rotor system subjected to axial excitation. Presence of axial excitation frequencies in the lateral vibration spectra represents the vibration coupling and thus a crack presence indicator. Moreover, numerical and experimental investigation of the dynamic behaviour of a cracked rotor system during start-up was carried out by El-Mongy et al [24] verified theoretical findings through experiments with a fatigue crack rotor.

Therefore, the number of the loops in the orbits at a given rotation speed can help to identify the critical speed of the cracked shaft. However, because the size of the loops depends on the crack depth [25]

A review of some previous techniques for modeling the open and the breathing crack models and the different methods of solution was introduced in [26]. the presence of cracks causes a local variation in the stiffness of the shaft of the rotor. The techniques used to formulate this variation, while using the FEM, are the flexibility matrix method and the method of the time-varying stiffness. The flexibility matrix method is the most common technique used to formulate the stiffness matrix of a cracked element of the rotor [27-30], The time-varying stiffness method which uses the formulas of the moments of inertia of an asymmetric rod in space is translated by a reduction of the moments of inertia around the axes of rotation of the cracked element, this method was used in [31,32] to study the model of the open cracks and in [33-35] to study the breathing cracks. Di et al. [36] studied the vibration response of a rotor

system with an elliptical crack. The cracked element stiffness was estimated based on the strain energy density approach that was described for the straight fronted crack [37].

In recent years, the hollow structures are widely used in aero-engine to improve efficiency. More attention is needed about the dynamic characteristics of cracked rotor system with hollow shaft in the engineering rotor [38,39]. the previous studies of cracked rotors show that the critical frequencies and the orbits as well as the amplitudes of the cracked rotor are slightly different from the uncracked rotor.

In our work, we use the classical version of FEM and the time-varying stiffness method to study the influence of breathing transverse crack on the orbits of the rotor centre during its passage through the subcritical speeds. This study makes it possible to determine the presence of cracks. A program that allows us to plot the orbit of the rotor centre of a cracked and uncracked rotor has been realized in MATLAB. This program is based on the non-linear method of Newmark. After the validation of our results, we study the orbit's behaviour according to the crack depth and according to the subcritical speeds.

## 2. Equation of Motion

The Jeffcott rotor model is studied in this work (rigid disk and flexible shaft). The equations of motion are obtained by the application of the Lagrange equation:

$$\frac{d}{dt} \left( \frac{\partial T}{\partial \dot{q}_i} \right) - \frac{\partial T}{\partial q_i} + \frac{\partial U}{\partial q_i} = F_i \quad (1)$$

Where:  $T$  - kinetic energy;  $U$  - Potential energy;  $F$  - External Forces;  $q$  - Generalized coordinates.

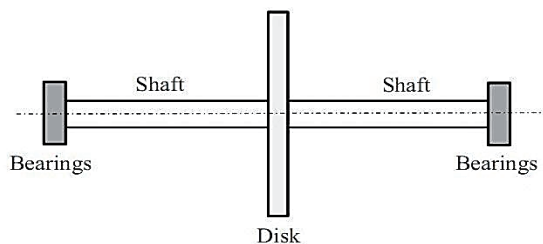


Figure 1: Model of a Jeffcott rotor.

### Kinetic energy of the disk

The expression of the kinetic energy of the disk is given by:

$$T_d = \frac{1}{2} m_d (\dot{u}^2 + \dot{w}^2) + \frac{1}{2} I_{dx} (\dot{\theta}_x^2 + \dot{\theta}_z^2) + \frac{1}{2} I_{dy} (\Omega^2 + 2\Omega \dot{\theta}_z \theta_x) \quad (2)$$

Where:  $\dot{u}$  and  $\dot{w}$  are the flexural velocities according to the X and Z axes of the fixed coordinates (OXYZ);  $\dot{\theta}_x$  and  $\dot{\theta}_z$  are the angular velocities according to the X and Z axes;  $m_d$  is the mass's disk;  $\Omega$  is the angular velocity;  $I_{dx}$ ,  $I_{dz}$  and  $I_{dy}$  are the moments of inertia of the disk, their expressions are given as:

$$I_{dx} = I_{dz} = \frac{m_d}{12} (3r^2 + 3R^2 + e^2) \quad (3)$$

$$I_{dy} = \frac{m_d}{12} (r^2 + R^2) \quad (4)$$

### Kinetic and strain energy of the shaft

The expression of the kinetic energy of an element of the shaft with a length  $L_e$  is given by:

$$T_a = \frac{1}{2} \rho_a S \int_0^{L_e} (\dot{u}^2 + \dot{w}^2) dy + \rho_a \frac{I_a}{2} \int_0^{L_e} (\dot{\theta}_x^2 + \dot{\theta}_z^2) dy + \rho_a I_a L_e \Omega^2 + 2\rho_a I_a \Omega \int_0^{L_e} \dot{\theta}_x \theta_z dy \quad (5)$$

The deformation energy of an element of the shaft is calculated by considering the case of an Euler-Bernoulli beam (shear deformation is negligible), this latter is given by:

$$U_a = \frac{E}{2} \int_0^{L_e} I_z \left( \frac{\partial \theta_z}{\partial y} \right)^2 + I_x \left( \frac{\partial \theta_x}{\partial y} \right)^2 + 2I_{xz} \frac{\partial \theta_z}{\partial y} \frac{\partial \theta_x}{\partial y} dy \quad (6)$$

In the case of an uncracked element, the moments of inertia of the cross section in the fixed coordinates are equal to  $I_x = I_z = \pi R^2 / 4$  and  $I_{xz} = 0$ .

In the case of cracked element and according to W.D. Pilkey [13], the moments of inertia of the cracked section in the fixed coordinates (Figure 1) are given by:

$$\begin{cases} I_x = I_x \sin^2 \Omega t + I_z \cos^2 \Omega t - 2I_{xz} \cos \Omega t \sin \Omega t \\ I_z = I_z \sin^2 \Omega t + I_x \cos^2 \Omega t - 2I_{xz} \cos \Omega t \sin \Omega t \\ I_{xz} = (I_x - I_z) \sin \Omega t \cos \Omega t - 2I_{xz} (\cos^2 \Omega t - \sin^2 \Omega t) \end{cases} \quad (7)$$

Where  $I_x$ ,  $I_z$  and  $I_{xz}$  are the moments of inertia of the uncracked section according to the rotating coordinates  $Oxyz$  (Figure 2), when  $\Omega t = -\pi/2$  (fully open crack), the expressions of these moments are given by [12] as:

$$\begin{cases} I_x = \frac{\pi R^4}{8} + \frac{R^4}{4} ((1-\mu)(2\mu^2 - 4\mu + 1)\gamma + \sin^{-1}(1-\mu)) \\ I_z = \frac{\pi R^4}{4} - \frac{R^4}{12} ((1-\mu)(2\mu^2 - 4\mu - 3)\gamma + 3\sin^{-1} \gamma) \\ I_{xz} = 0 \end{cases} \quad (8)$$

Where  $\mu = h/R$  is the ratio between the crack depth and the radius of the shaft ( $0 \leq \mu \leq 1$ ) and  $\gamma = \sqrt{\mu(2-\mu)}$ .

In the case of breathing cracks, the expressions of the moments of inertia of the cracked element (uncracked section); (Figure 2); during the rotation are given as:

$$\begin{cases} I_x = \left( \frac{I_a - I_x}{2} \right) \sin(\Omega t) + \left( \frac{I_a + I_x}{2} \right) \\ I_z = \left( \frac{I_a - I_z}{2} \right) \sin(\Omega t) + \left( \frac{I_a + I_z}{2} \right) \end{cases} \quad (9)$$

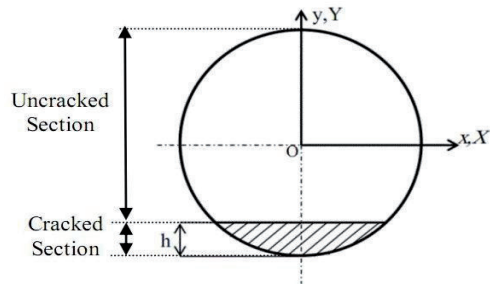


Figure 2: Cross-section of the cracked element.

Figure 3 shows the variation of the stiffness of the cracked element with respect to the rotational angle ( $\Omega t$ ), that means the time-varying stiffness.

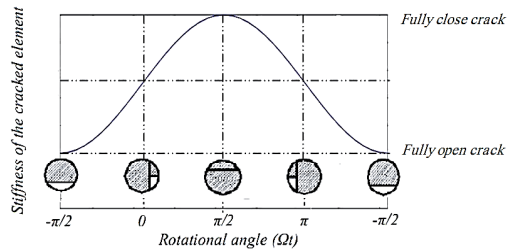


Figure 3: Variation of the stiffness of the cracked element with respect to the rotational angle ( $\Omega t$ ).

Figures 4 and 5 represent the of variation curves of  $I_x$ ,  $I_z$ , et  $I_{xz}$  according to rotational angle ( $\Omega t$ ) in the case where  $\mu = 0.5$ . These figures show that, for:

–  $\Omega t = \pi/2$ ; where the crack is totally close;  $I_x$ ,  $I_z$  take the value of the moments of inertia of uncracked section ( $I_a$ ).

–  $\Omega t = -\pi/2$ ; where the crack is totally open;  $I_z$  is greater than  $I_x$ , this is because the asymmetry of the cross section.

–  $\Omega t = \pi/2$ ,  $\Omega t = \pi/4$ ,  $\Omega t = 3\pi/4$ ,  $\Omega t = -\pi/4$  and  $\Omega t = -3\pi/4$  the cross section is symmetric according the X and Z axes, therefore  $I_x = I_z$  and  $I_{xz} = 0$ .

Figures 6-8 represent the variation curves of  $I_x$ ,  $I_z$  and  $I_{xz}$  for  $R = 0.795 \times 10^{-3}$  m with different values of  $\mu$ ; from these figures we can see that the stiffness of the shaft decrease with the increase of the crack depth, this variation is periodic during its rotation (time varying stiffness).

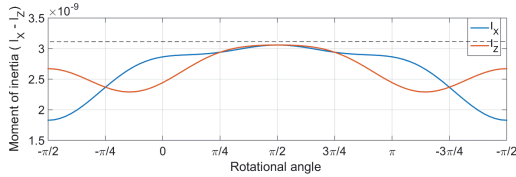


Figure 4: Variation curve of  $I_x$  and  $I_z$  according to rotational angle ( $\Omega t$ ).

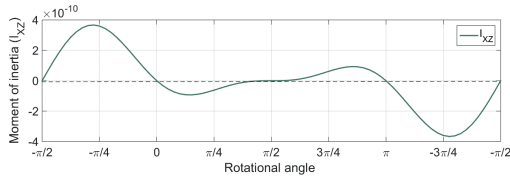
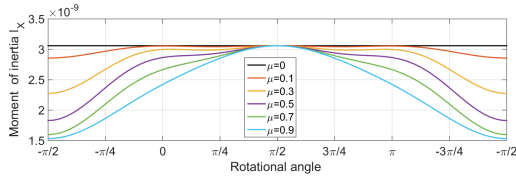
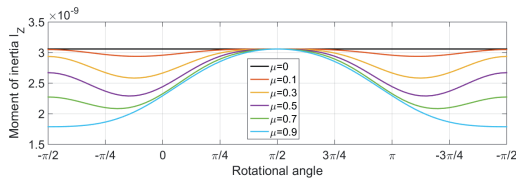


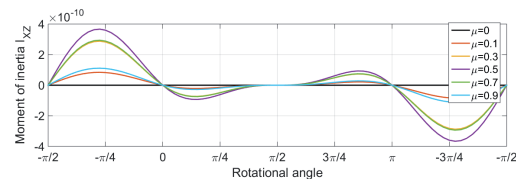
Figure 5: Variation curve of  $I_{xz}$  according to rotational angle ( $\Omega t$ ).



Figures 6: Variation curve of  $I_x$  with different value of crack depth ( $\mu$ ).



Figures 7: Variation curve of  $I_z$  with different value of crack depth ( $\mu$ ).



Figures 8: Variation curve of  $I_{xz}$  with different value of crack depth ( $\mu$ ).

## Generalized forces of the bearings

The components of the generalized forces of the bearings  $F_u$  and  $F_w$  along the X and Z axes are given as:

$$\begin{bmatrix} F_u \\ F_w \end{bmatrix} = - \begin{bmatrix} k_{xx} & k_{xz} \\ k_{zx} & k_{zz} \end{bmatrix} \begin{bmatrix} u \\ w \end{bmatrix} - \begin{bmatrix} c_{xx} & c_{xz} \\ c_{zx} & c_{zz} \end{bmatrix} \begin{bmatrix} \dot{u} \\ \dot{w} \end{bmatrix} \quad (10)$$

## Kinetic energy of the unbalance

The unbalance is characterized by its kinetic energy given by:

$$T_b = m_b d \Omega^2 (\dot{u} \sin(\Omega t + \beta) - \dot{w} \cos(\Omega t + \beta)) \quad (11)$$

Where:  $m_b$  - is the mass of the unbalance;  $d$  - is the distance between the position of the unbalance mass and the centre;  $\beta$  - is the angle with respect to Z axis.

## 2. Matrix Formulation

We use the classical version of the FEM to determine the global matrices of the equation of motion [11]:

$$[M_g] \ddot{q} + ([C_p] + \Omega [G_g]) \dot{q} + ([K_p] + [K_g]) q = F_b \quad (12)$$

Where:  $[M_g]$  is the global mass matrix which comprises the mass matrix of the disk and the shaft;  $[G_g]$  is the global gyroscopic matrix that includes the gyroscopic matrix of the disk and the shaft;  $[K_g]$  is the global stiffness matrix of the shaft which comprises the stiffness matrix of the cracked element assembled with the matrices of other elements replacing the matrix of the healthy element by the matrix of cracked element;  $[C_p]$  and  $[K_p]$  are the damping and stiffness matrices of the bearings;  $q$  is the vector of generalized coordinates;  $F_b$  is the vector of unbalance forces;  $\Omega$  is the rotation speed in rad/s.

## 3. Validation

Figure 9 shows the finite element model of the rotor studied by Al-Shudeifat [8], the rotor is discretized into 12 elements, and the physical parameters of this rotor are presented in table 1.

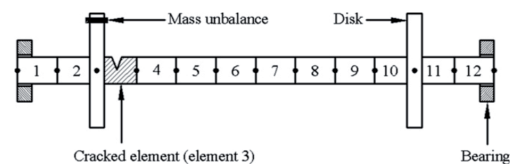


Figure 9: Finite element model of the studied rotor [8].

Table 1: Physical parameters of the studied rotor.

Young's Module (E)	2.1e11 N/m <sup>2</sup>
Length of the shaft (L)	0.65 m
Density of the shaft ( $\rho_a$ )	7800 kg/m <sup>3</sup> (Steel)
Position of the disk 1	0.124 m (from the left bearings)
Position of the disk 2	0.6 m (from the left bearings)
Inner radius of the disks (R)	0.795e <sup>-3</sup> m
External radius of the disks (r)	76.2e <sup>-3</sup> m
Thickness of the disks (e)	11.72e <sup>-3</sup> m
Density of the disk ( $\rho_d$ )	2700 kg/m <sup>3</sup> (Aluminium)
Stiffness of bearings ( $k_{ax}, k_{az}$ )	7e <sup>7</sup> N/m
Damping of bearings ( $c_{ax}, c_{az}$ )	5e <sup>2</sup> Ns/m
Mass unbalance ( $m \cdot d^2$ )	10 <sup>-3</sup> kg.m <sup>2</sup>
Mass unbalance angle	$\pi/2$ rad

To improve the efficiency of our program, we compare our results with those experimental results of Al-shudeifat's [16].

Figure 10 shows our theoretical orbits (Blue) and the Al-shudeifat's experimental orbits (Black) of node 2 of the studied rotor during its passage through the first backward (a) and forward (b) subcritical speed in the case where  $\mu=0.48$ ; knowing that the first backward speed  $\omega_{b1}=2850$  rpm and the first forward speed  $\omega_{f1}=3007$  rpm. From this Figure, we can see a clearly identification of amplitudes and orbits shape of our results and the experimental of Al-shudeifat's [16].

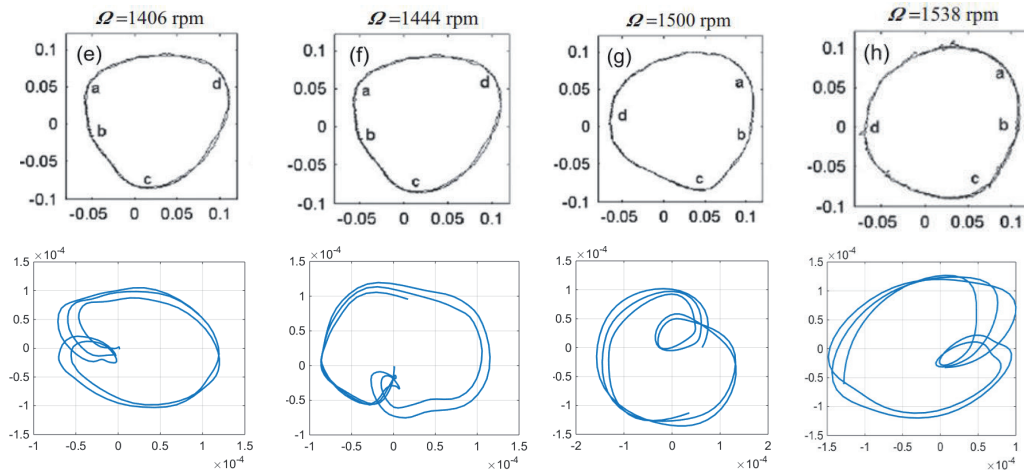


Figure 10: Experimental and theoretical orbits of the studied rotor during its passage through the first backward (a) and forward (b) subcritical speed.

## 4. Result and Discussion

In this part of our work, we study the orbit's behaviour according to the crack depth and according to the subcritical speeds.

Figure 11 shows the variation of orbits of node 2 during its passage through the first subcritical forward speed ( $1/2 \omega_{f1} \approx 1500$  rpm) for different values of the crack depth. An inner loop appears in the orbit of the cracked shaft compared to the intact shaft where its circumference increase with the propagation of the crack.

Figure 11 shows the variation of orbits of node 8 during its passage through the first, second, third and the fourth subcritical forward speeds ( $1/2 \omega_{f1} \approx 1500$  rpm ;  $1/3 \omega_{f1} \approx 1000$  rpm;  $1/4 \omega_{f1} \approx 750$  rpm;  $1/5 \omega_{f1} \approx 600$  rpm) where the non-dimensional crack depth  $\mu=0.6$ . From this figures; more inner loops appear for the second, third and the fourth subcritical speeds.

## 5. Conclusion

In this work, we are studied the influence of a transverse breathing crack on the orbits of a rotor during its passage through the subcritical speeds; a program based on the method of Newmark beta was developed in MATLAB. Our results are compared with an experimental work. From our results, we can notice that:

- » Inner loops appear on the orbits due to the presence of a breathing crack.
- » The inner loop evolves with the increase of the crack depth
- » The inner loops evolve when the rotor turns through its

subcritical speeds.

» More inner loops appear when the rotor turns through its second and third subcritical speeds.

» The orientation of the inner loops changes during the rotation of the rotor.

» As the rotor speed increase the inner loops evolves.

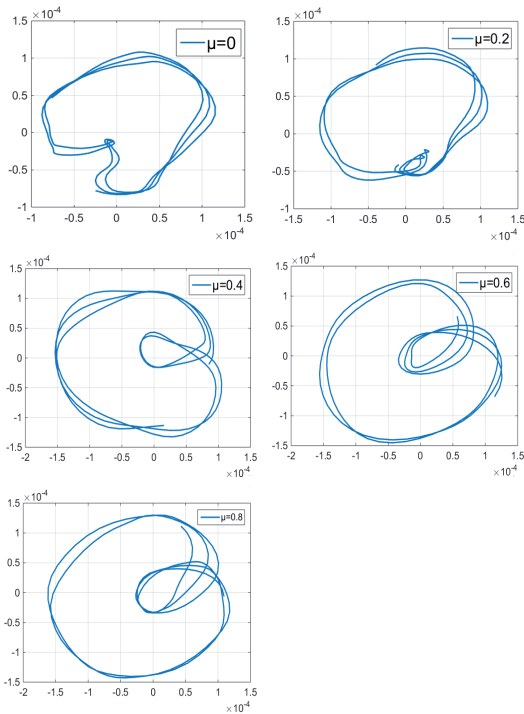


Figure 11: Orbits of node 2 for different values of crack depth ( $\mu$ ).

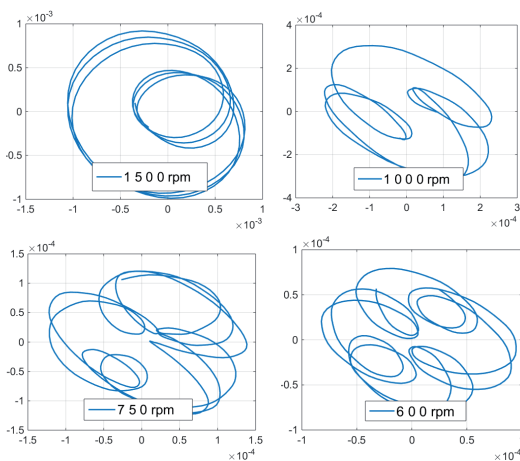


Figure 12: Orbits of node 8 through the first forward subcritical speed.

## References

- [1] J. Wauer, "Dynamics of cracked rotors: literature survey". Appl. Mech. Rev., 43:13–7, 1990.
- [2] A. Dimarogonas, "Vibration of cracked structures: a state of the art review". Eng. Fract. Mech., 55:831–57, 1996.
- [3] G. Sabnavis, and Kirk RG, Kasarda M, Quinn D, "Cracked shaft detection and diagnostics: a literature review". Shock Vibr Digest, 36(4):287–96, 2004.
- [4] A. S. Sekhar, B. S. Prabhu, Transient analysis of a cracked rotor passing through critical speeds, Journal of Sound and Vibration, 173(3) (1994) 415–421.
- [5] A. S. Sekhar, Crack identification in a rotor system: a model-based approach, Journal of Sound and Vibration, 270 (2004) 887–902.
- [6] A. S. Sekhar, A. R. Monhanty, S. Prabhakar, Vibration of cracked rotor system: transverse crack versus slant crack, Journal of Sound and Vibration, 279 (2005) 1203–1217.
- [7] A. K. Darpe, A novel way to detect transverse surface crack in a rotating shaft, Journal of Sound and Vibration, 305 (2007) 151–171.
- [8] A. S. Sekhar, B. S. Prabhu, Transient analysis of a cracked rotor passing through critical speed, Journal of Sound and Vibration, 173 (3) (1994), 415–421.
- [9] A. S. Sekhar, B. S. Prabhu, Vibration and stress fluctuation in cracked shafts, Journal of Sound and Vibration, 169 (5) (1994), 655–667.
- [10] L. Xiang, Y. Zhang, A. Hu, Crack characteristic analysis of multi-fault rotor system based on whirl orbits, Nonlinear Dyn 95 (2019) 2675–2690, <https://doi.org/10.1007/s11071-018-4715-y>.
- [11] A.D. Nembhard, J.K. Sinha, A. Yunusa-Kaltungo, Experimental observations in the shaft orbits of relatively flexible machines with different rotor related faults, Meas. J. Int. Meas. Confed. 75 (2015) 320–337, <https://doi.org/10.1016/j.measurement.2015.08.007>
- [12] Al-Shudeifat MA, Butcher EA (2011) New breathing functions for the transverse breathing crack of the cracked rotor system: approach for critical and subcritical harmonic analysis. J Sound Vib 330(3):526–544.
- [13] R. Gasch, Dynamic behaviour of a simple rotor with a cross-sectional crack, Vibration in Rotating Machinery, Institution of Mechanical Engineers, London, 1976, pp. 123–128.
- [14] G.B. Thomas, The application of non-linear methods to turbo-generator rotordynamics, Vibration in Rotating Machinery, Institution of Mechanical Engineers, London, 1979, pp. 209–216.
- [15] I.W. Mayes, W.G.R. Davies, A method of calculating the vibrational behaviour of coupled rotating shafts containing a transverse crack, Vibration in Rotating Machinery, Institution of Mechanical Engineers, London, 1980, pp. 17–



- 27.
- [16] I.W. Mayes, W.G.R. Davies, Analysis of the response of a multi-rotor-bearing system containing a transverse crack in a rotor, *Journal of Vibration, Stress, and Reliability in Design—Transactions of the ASME* 106 (1984) 139–145.
- [17] O.S. Jun, H.J. Eun, Y.Y. Earmme, C.-W. Lee, Modelling and vibration analysis of a simple rotor with a breathing crack, *Journal of Sound and Vibration* 155 (1992) 273–290.
- [18] J J Sinou, A W Lees. A non-linear study of a cracked rotor. *European Journal of Mechanics A/Solids*, 2007, 26: 152–170
- [19] I. Green, C. Casy, Crack detection in a rotor dynamic system by vibration monitoring - Part I: Analysis, *Journal of Engineering for Gas Turbine and Power*, 127 (2005) 425–436.
- [20] O. S. Jun, M. S. Gadala, Dynamic behavior analysis of cracked rotor, *Journal of Sound and Vibration*, 309 (2008) 210–245.
- [21] L. Xiao-feng, X. Ping-yong, S. Tie-lin, Y. Shu-zi, Nonlinear analysis of a cracked rotor with whirling, *Applied Mathematics and Mechanics*, 23 (2002) 721–731.
- [22] C. M. Stoisser, S. Audebert, A comprehensive theoretical, numerical and experimental approach for crack detection in power plant rotating machinery, *Mechanical Systems and Signal Processing*, 22 (2008) 818–844.
- [23] El-Mongy HH, Younes YK, El-Morsy MS (2015) Vibrational characteristics of a cracked rotor subjected to periodic auxiliary axial excitation. In: *Vibration engineering and technology of machinery*, Springer, pp 777–787.
- [24] A K Darpe, K Gupta, A Chawla. Transient response and breathing behaviour of a cracked Jeffcott rotor. *Journal of Sound and Vibration*, 2004, 272: 207–243
- [25] Sinou, J.J.; Lees, A.W. The influence of cracks in rotating shafts. *J. Sound Vib.* 2005, 285, 1015–1037. [CrossRef]
- [26] C. A. Papadopoulos, The strain energy release approach for modeling cracks in rotors: a state of the art review, *Mechanical Systems and Signal Processing*, 22 (2008) 763–789
- [27] C.A. Papadopoulos, A.D. Dimarogonas, “Coupled longitudinal and vertical vibrations of a rotating shaft with an open crack”, *Journal of Sound and Vibration*, 117 (1) 81–93. 1987.
- [28] A.C. Chasalevris, C.A. Papadopoulos, “Coupled horizontal and vertical bending vibrations of stationary shaft with two cracks”, *Journal of Sound and Vibration*, 309 507–528, 2007.
- [29] A.S. Sekhar, B.S. Prabhu, “Transient analysis of a cracked rotor passing through critical speeds”, *Journal of Sound and Vibration*, 173 (3) 415–421, 1994.
- [30] A.S. Sekhar, “Crack identification in a rotor system: a model-based approach”, *Journal of Sound and Vibration*, 270 887–902, 2004.
- [31] M.A. AL-Shudeifat, “On the finite element modeling of an asymmetric cracked rotor”, *Journal of Sound and Vibration*, 332 (11) 2795–2807, 2013.
- [32] M.A. AL-Shudeifat, “Stability analysis and backward whirl investigation of cracked rotors with time-varying stiffness”, *Journal of Sound and Vibration*, 348 365–380, 2015.
- [33] J.-J. Sinou, and A.W. Lees, “The influence of cracks in rotating shafts”, *Journal of Sound and Vibration*, Volume 285, Issues 4-5, 1015-1037, August 2005.
- [34] M.A. AL-shudeifat, E.A. Butcher, C.R. Stern, “General harmonic balance solution of a cracked rotor-bearing-disk system for harmonic and sub-harmonic analysis: analytical and experimental approach”, *International Journal of Engineering Science*, 48 (10) 921–935, 2010.
- [35] M.A. AL-Shudeifat, and E.A. Butcher, “New breathing functions for the transverse breathing crack of the cracked rotor system: approach for critical and subcritical harmonic analysis”, *Journal of Sound and Vibration*, 330 (3) 526–544, 2011.
- [36] Di Y, Liu CL, Zhang QD, Cheng W, Zhou, SP (2012) Dynamic analysis of the rotor system with a semi-elliptical fronted crack on the shaft. In: *Applied Mechanics and Materials*, Trans Tech Publications Ltd., Vol. 226, pp. 665–671
- [37] Dimarogonas AD, Paipetis SA, Chondros TG (2013) *Analytical methods in rotor dynamics*. Springer Science & Business Media, Berlin
- [38] Lu ZY, Hou L, Chen YS, et al. Nonlinear response analysis for a dual-rotor system with a breathing transverse crack in the hollow shaft. *Nonlin Dyn* 2016; 83: 169–185.
- [39] Guo CZ, Al-Shudeifat MA, Vakakis AF, et al. Vibration reduction in unbalanced hollow rotor systems with nonlinear energy sinks. *Nonlin Dyn* 2015; 79: 527–538.